Domain boundary pinning and elastic softening in $KMnF_3$ and $KMn_{1-x}Ca_xF_3$

2009 J. Phys.: Condens. Matter 21 035901

(http://iopscience.iop.org/0953-8984/21/3/035901)

J. Phys.: Condens. Matter **21** (2009) 035901 (7pp) doi:10.1088/0953-8984/21/3/035901

Domain boundary pinning and elastic softening in $KMnF_3$ and $KMn_{1-x}Ca_xF_3$

Ekhard K H Salje[1] **and Huali Zhang**

Department of Earth Sciences, University of Cambridge, Downing Street, Cambridge CB2 3EQ, UK

Received 30 September 2008, in final form 21 November 2008
Published 11 December 2008
Online at stacks.iop.org/JPhysCM/21/035901

Abstract

Anelastic softening related to the movement of twin boundaries is observed in improper ferroelastic $KMnF_3$ and $KMn_{1-x}Ca_xF_3$. Wall movement in $KMnF_3$ shows a frequency dependence which is described in terms of an extended Debye relaxation with an extension exponent of 0.54. This exponent indicates a fairly narrow distribution of activation energies near 0.43 eV. Wall movements in Ca-doped samples are best described in terms of Vogel–Fulcher (VF) relaxations with a VF energy of 0.23 eV. The activation energies are related to interaction between F vacancies or interstitials and the moving domain walls; Ca doping appears to increase the tendency to form glass-like states. No domain freezing occurs at temperatures above the subsequent phase transition $I4/mcm$–$Pnma$; the $Pnma$ phase does not show any domain movement and anelastic behaviour. Elastic precursor softening is observed above the transition temperature between the cubic and the tetragonal phase. The softening can be described empirically using a power law: $[(T - T_o)/T_o]^{-K}$ with values of the exponent K around 0.5.

(Some figures in this article are in colour only in the electronic version)

1. Introduction

Ferroelastic and martensitic materials often show significant elastic softening and anelastic behaviour when subjected to external stresses [1–9]. Such anelasticity is related to the movement of twin boundaries. Anelasticity is related to the extension and retraction of individual needle domains [4] for weak stress fields and the sideward movement of twin boundaries is also observed for stronger stress fields. Hindrance to this movement is given by pinning centres [2–5, 8] and boundary conditions [10]. However, Lee *et al* [11] have argued that intrinsic pinning via the Peierls lattice effect is only physically possible if the thickness of the twin wall is sufficiently small, i.e. narrow walls are more likely to be pinned than diffuse walls. Narrow walls occur in many metallic shape memory alloys while in ferroelastic perovskites, as example, the wall thickness expands to several nanometres. Such walls are less likely to be pinned by the Peierls lattice effect. In the latter group of materials the pinning can only occur via extrinsic defects, boundaries or interactions with other twin walls, dislocations etc. Mobile defects can be transported with the wall movement and only freeze out at very low temperatures. Such effects are also important for the investigation of the propagation and damping of seismic waves where the amplitudes are extremely small (10^{-8} in the far field) and the frequencies are low (below 1 Hz) [2–5].

Experimentally, pinning effects have been observed in $LaAlO_3$ [2–4] and $Ca_{1-x}Sr_xTiO_3$ [5]. In $Ca_{1-x}Sr_xTiO_3$ [5], oxygen vacancies or clusters of such vacancies [11] pin the domain wall at 423 K for $0.68 < x < 0.9$. The activation energy for the wall movement is 0.8 eV which is characteristic for oxygen vacancies [5, 12]. In $LaAlO_3$ the freezing temperature is 423 K with an activation energy of 0.88 eV [2, 4]. No activated process was found in $SrTiO_3$ [6] and $KMnF_3$ [7]. In these materials twin walls appear to remain mobile to the lowest temperature measured. We have to assume, therefore, that the defects either travel with the moving domain wall or that the pinning force is weak enough so that the wall movement is not impeded by defects at low frequencies (between 0.2 and 32 Hz).

This study is, to our knowledge, the first to focus on fluoroperovskites. There are two reasons for using a perovskite based on fluorine octahedra rather than the more common oxygen octahedra. First, it appears that in oxides the pinning of domain walls is largely attributed to oxygen vacancies [2, 4, 5, 12]. However, the internal wall structure

[1] On leave to: Max Planck Institute for Mathematics in the Sciences/Leipzig, Germany.

in oxides can be complex with secondary order parameters located inside the walls but not in the bulk [13, 14]. As an example may serve $CaTiO_3$ where twin walls contain electric dipole moments while no such dipole moments exist in the ferroelastic bulk [14]. Such local wall structures can give rise to pinning mechanisms which go beyond the standard pinning models [1, 11, 15]. The question arises whether F-based perovskites with similar structural deformations in the bulk show domain freezing related to such secondary order parameters.

The second reason for choosing $KMn_{1-x}Ca_xF_3$ is to test the validity of the results of Cao and Barsch [16] who reported precursor softening in $KMnF_3$ at temperatures above the transition point to the paraelastic phase as measured by ultrasonic high frequency experiments. These authors argued convincingly that the tilt transformation in $KMnF_3$ is not a rigid body transition but that the anharmonicity of the structure is related to the atomic Mn–F interaction while all other interactions appear to be less important. The same line of argument was used for $SrTiO_3$ [17–20] where the anomaly arises from the highly non-linear polarization of the oxygen ions. Equivalently it was shown that the transition in $KMnF_3$ is due to the specific properties of the Mn–F interaction and not due to the space filling effect of K. Precursor softening of the elastic moduli C_{11}, C_{12} and C_{44} was observed between T_o and $T_o + 150$ K.

Similar softening (called a cusp-like anomaly by Cao and Barsch [16]) has already been studied in oxide perovskites [21–23] and other materials [24]. This softening can be described empirically by a power law with an exponent K (other symbols have been used previously. Here we follow the notation of [24] in order to avoid confusion with the critical exponent δ). We have compared our results in $KMnF_3$ with those of Cao and Barsch [16] and find that in our low frequency measurements (0.2–32 Hz) the anomaly is limited to a much smaller temperature interval so that the conclusions drawn previous cannot be universal and hence a structural interpretation appears to be more difficult than previously anticipated [16].

Finally we will show that no anelastic effect exists in the $Pnma$ phase so that we argue that no stress induced movement of twin walls appears to happen in that phase [25, 26].

2. Phase transition in $KMn_{1-x}Ca_xF_3$

Pure $KMnF_3$ undergoes several phase transitions at the following temperatures: 186.5, 88 and 82 K [27]. The first transition, which is slightly first order, occurs at around $T_{c1} =$ 186.5 K and corresponds to the softening of phonons having the R_{25} symmetry. The high temperature cubic space group is $Pm3m$ which transforms to $I4/mcm$ with the tetragonal c-axis developing around the [001] cubic axis. The second transition at $T_{c2} = 88$ K is from a tetragonal to an orthorhombic phase ($Pnma$) although the details of the transition mechanism is not clear. An alternative space group may be $Cmcm$ which would maintain the tilt system of the $I4/mcm$ phase. Finally, below $T_{c3} = 82$ K, a tetragonal (or monoclinic) phase develops [27].

For the Ca-doped samples, the temperatures of these three structural phase transitions are enhanced when Mn^{2+} ions are substituted by Ca^{2+} ions. The increase per % of Ca for the three phase transitions are 5.8, 18, and 14 K, respectively [27].

$KMnF_3$ becomes anti-ferromagnetic below the Néel temperature $T_N = 88$ K and transforms further to a canted antiferromagnet at 82 K. According to various authors, an additional structural phase transition may exist at 91 K. This transition was reported to be either first order [28] or second order [29]. Kapusta *et al* [30] claimed the 91 K transition to be a tetragonal/monoclinic transition while Gibaud *et al* [27] and Salazar *et al* [31] do not observe any anomaly at this temperature. In our experiments we cannot reach temperature below 100 K so that we can only investigate the phases I $4/mcm$ and, for Ca-doped samples, $Pnma$.

3. Experimental procedures

Samples of $KMn_{1-x}Ca_xF_3$ were prepared at University du Maine (Le Mans, France) using the Bridgman–Stockbarger method. The chemical characteristics of the samples were examined using an electron microprobe CAMECA SX50. The pure $KMnF_3$ sample did not show any trace of calcium. The doped samples showed Ca concentration of 0.3 mol%, 1.7% and 2.3%. The microanalysis experiments showed slight inhomogeneities in the composition of the doped samples, for example, the composition of the fourth sample is 2.30% ± 0.13%.

The samples for dynamical mechanical analysis (DMA) experiments with size around $1 \times 1 \times 7$ mm^3 were cut using a high-speed saw from the big single crystals. The three edge directions of the DMA samples are all parallel to [100] of the cubic phase. Mechanical properties were measured using a Perkin–Elmer dynamical mechanical analyzer (DMA-7e) operating in three-point bend geometry. The sample was suspended on two knife edges, 5 mm apart. A force is applied from above via a third knife edge located halfway between the supporting knives. The total force is the sum of a static component F_S and a dynamic component with amplitude F_D and frequency f. The amplitude of deflection (u_D) and phase lag (ϕ) are measured with resolutions of Δu_D around 10 nm and $\Delta\phi = 0.1°$, respectively. The dynamic Young's modulus is

$$E = \frac{l^3}{4t^3 w}\frac{F_D}{u_D}\exp(i\phi) \tag{1}$$

while l, w and t are the distance between knife edges, the width and the thickness of the sample, respectively. The real ($E' = |E|\cos(\phi)$) and imaginary ($E'' = |E|\sin(\phi)$) parts of the dynamic modulus are referred to as the storage and loss modulus, respectively. The ratio $E''/E' = \tan(\phi)$ is the mechanical loss (energy dissipated per cycle). DMA experiments were performed with various frequencies and $F_S = 110$ mN, $F_D = 100$ mN. The temperature was changed between room temperature and 100 K with a heating/cooling rate of $\dot{T} = 2$ K min^{-1}. Precursor softening, was measured using larger forces in order to reduce the experimental noise; the deflection amplitude in the cubic phase was ca 1 μm.

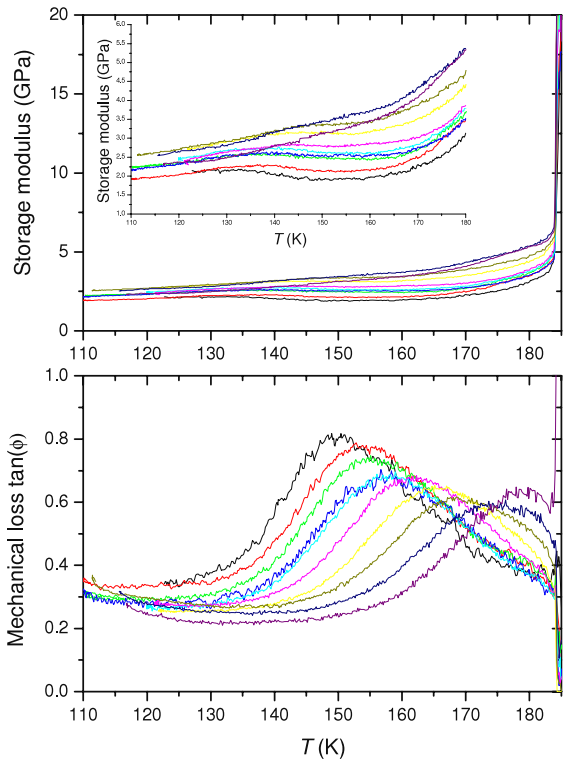

Figure 1. Storage modulus and mechanical loss of $KMnF_3$. The frequencies from bottom to top at 170 K for moduli and from left to right for mechanical loss peaks are 0.2, 0.4, 0.6, 0.8, 1, 2, 4, 8, 16, 32 Hz.

4. Results

The ferroelastic phase transition cubic–tetragonal is clearly visible in all experiments by a drop of the storage modulus by a factor of 3 or more. This clearly shows the effect of mobile domain boundaries in the tetragonal phase. In no sample did we observe strong domain boundary freezing at lower temperatures (in contrast with the behaviour of $LaAlO_3$ [4]). Instead we find a massive increase of the elastic stiffness near the phase transition tetragonal–orthorhombic. No indication for any wall movement was found in the orthorhombic *Pnma* phase. This behaviour is similar to $Ca_{1-x}Sr_xTiO_3$ where the *Pnma* phase is also as stiff as the paraphase *Pm*3*m* [5, 25, 26].

In detail, we show in figure 1 the temperature dependence of the storage modulus and mechanical loss of $KMnF_3$. The phase transition at 184 K appears as a large decrease of the storage modulus on cooling. Twin domain walls form below the transition and the domain wall can move in response to an applied stress so the modulus rapidly decreases to a value about one fourth of the cubic phase and remains almost constant when temperature is lowered further. Below 184 K some mechanical loss is observed, accompanied by a corresponding small decrease of the storage modulus which can be seen in the inserted figure of figure 1. The peak shifts to higher temperature with increasing frequency, which demonstrates that the relaxation process is thermally activated. We fit the temperature evolution of the mechanical loss to an Arrhenius expression $\tau = \tau_0 \exp(E_a/kT)$, where τ is the relaxation time,

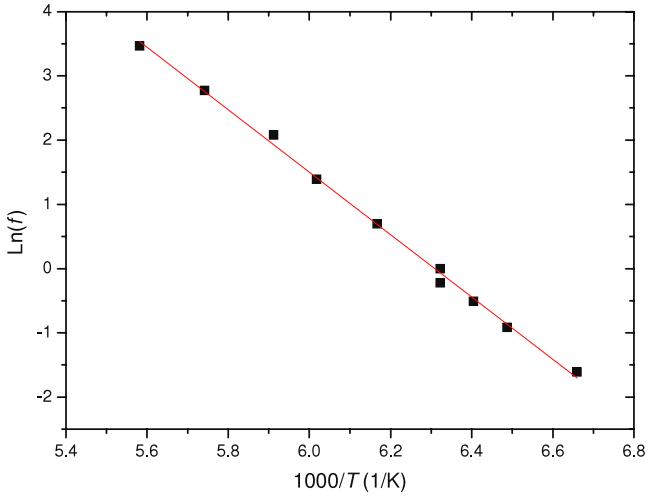

Figure 2. Ln (f) versus $1/T$ for $KMnF_3$.

τ_0 is the relaxation time extrapolated to infinite temperature and E_a is the activation energy. With $\omega = 2\pi f$, the peak position is given by $\ln(2\pi f\tau_0) + E_a/kT = 0$. The $\ln(f)$ versus $1/T$ curve shown in figure 2 gives $E_a = 0.43$ eV and $\tau_0 = 8 \times 10^{-15}$ s. Debye relaxations usually do not describe wall movements quantitatively so that either extended Debye expressions or stochastic equations are used for the analysis [8]. Here we use the generalized Debye equation

$$J(\omega) = J_1 - iJ_2 = J_U + \frac{\Delta J}{1 + i(\omega\tau)^u} \tag{2}$$

$$J_1 = J_U + \frac{\Delta J}{1 + (\omega\tau)^{2u}} \tag{3}$$

$$J_2 = \Delta J \frac{(\omega\tau)^u}{1 + (\omega\tau)^{2u}} \tag{4}$$

where J_U is the unrelaxed compliance (i.e. the instantaneous elastic response of the lattice), ΔJ is the anelastic contribution to the compliance and u is the broadening exponent. The mechanical loss are related to the compliance via

$$\tan(\phi) = \frac{J_2}{J_1}. \tag{5}$$

Combined with the relaxation time $\tau = \tau_0 \exp(E_a/kT)$, the fitting of the experimental data of mechanical loss of pure $KMnF_3$ for $f = 1$ Hz with equations (2)–(5) as function of temperature is shown in figure 3. This analysis allows for a spread of the activation energy of 0.43 eV over a narrow distribution [4] which is plausible for weakly heterogeneous materials ($u = 0.54$, $J_U/\Delta J = 0.77$, $\tau_0 = 7 \times 10^{-15}$ s).

Figure 4 shows the temperature dependence of the storage modulus and mechanical loss of $KMn_{0.997}Ca_{0.003}F_3$. The modulus drops at the temperature of the cubic–tetragonal phase transition and a mechanical loss peak is observed below the phase transition. The change of the modulus is too small to be seen. Through the $\ln(f)$ versus $1/T$ curve, we obtained $E_a = 0.68$ eV and $\tau_0 = 2 \times 10^{-22}$ s. The value of τ_0 is far too low compared with the values characteristic for atomic hopping

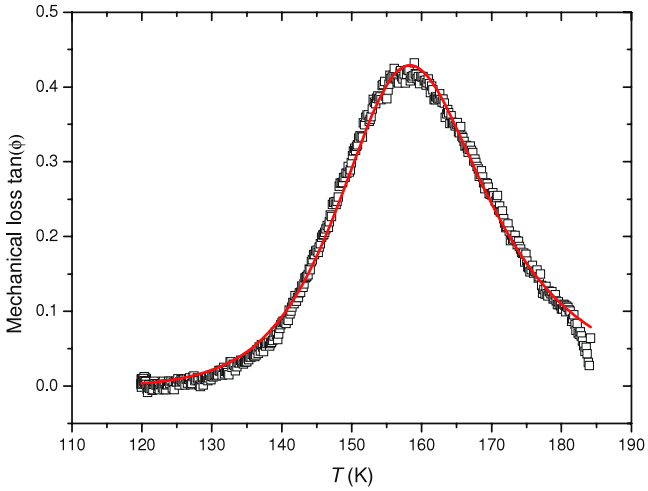

Figure 3. Mechanical loss of $KMnF_3$ for $f = 1$ Hz as a function of temperature and the fitted curve of the extended Debye model (equations (2)–(5)).

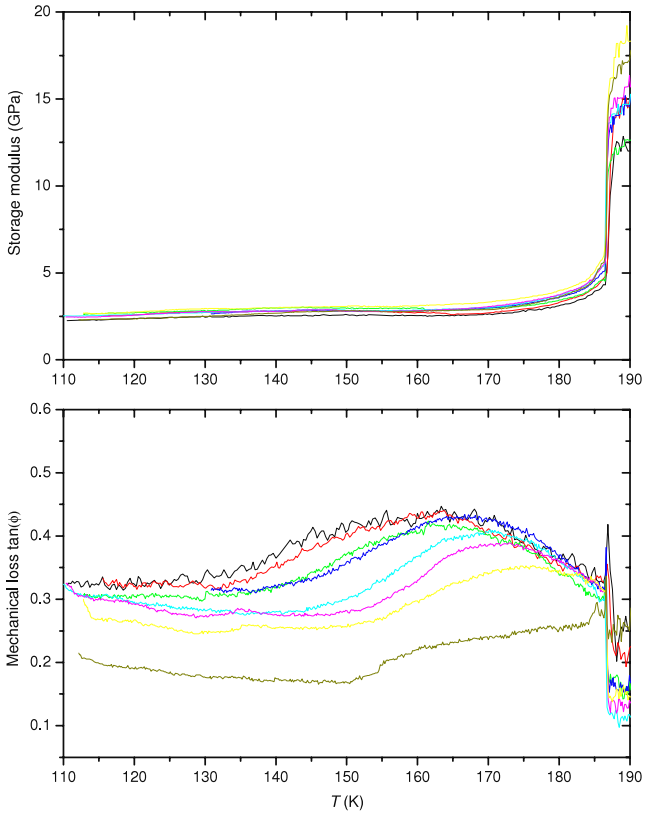

Figure 4. Storage modulus and mechanical loss of $KMn_{0.997}Ca_{0.003}F_3$. The frequencies are 0.2, 0.4, 1, 2, 4, 8, 16, 32 Hz and raise from bottom to top at 182 K for the moduli and from left to right for the mechanical loss peaks.

pointing to a glass transition process [32]. Therefore we fit our data with a Vogel–Fulcher relaxation $\tau = \tau_0 \exp(E_a/k(T - T_f))$ with freezing temperature $T_f = 70$ K which results in $E_a = 0.23$ eV, $\tau_0 = 8 \times 10^{-14}$ s (figure 5). The fit is not quite accurate as the value of T_f is rather un-constrained. The fitting of the mechanical loss peak with equations (2)–(5) and

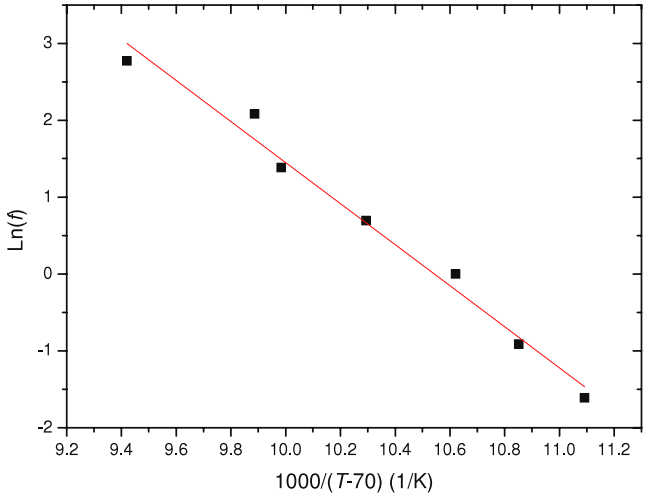

Figure 5. Ln (f) versus $1/(T - 70)$ for $KMn_{0.997}Ca_{0.003}F_3$.

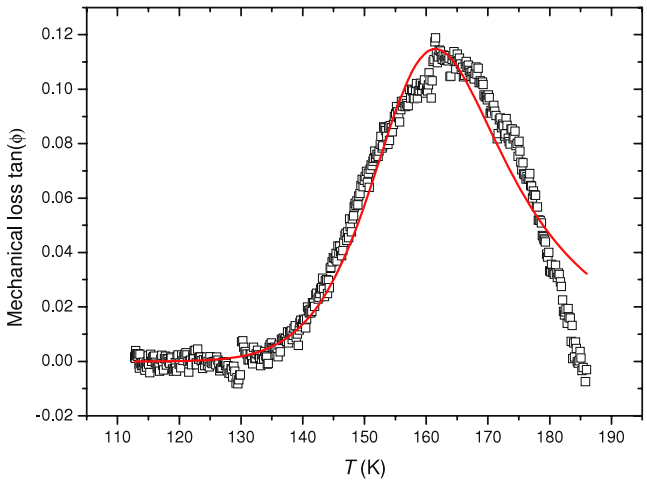

Figure 6. Mechanical loss of $KMn_{0.997}Ca_{0.003}F_3$ for $f = 1$ Hz as a function of temperature and the fitting line of the extended Debye model (equations (2)–(5)).

Table 1. Parameters of the extended Debye model for $KMn_{0.997}Ca_{0.003}F_3$.

T_f (K)	E_a (eV)	τ_0 (s)	$J_U/\Delta J$	u
70	0.23	3×10^{-14}	3.9	0.31

Vogel–Fulcher relaxation law is shown in figure 6 with parameters listed in table 1.

The storage moduli for $KMn_{0.983}Ca_{0.017}F_3$ and $KMn_{0.977}Ca_{0.023}F_3$ are shown in figure 7. The softening of the modulus at the cubic to tetragonal phase transition is similar as in $KMnF_3$ and $KMn_{0.997}Ca_{0.003}F_3$. A massive increase of the elastic stiffness is observed near the phase transition tetragonal–orthorhombic. The transition temperatures agree well with those reported by Gibaud *et al* [27]. They also reported another phase transition below the tetragonal–orthorhombic transition although we observed no additional anomaly in $KMn_{0.983}Ca_{0.017}F_3$ and $KMn_{0.977}Ca_{0.023}F_3$.

We now turn to the measurement of the precursor softening above the temperature of the cubic/tetragonal transition.

Table 2. Parameters of the power law fitting for the relative softening above the phase transition $Pm3m$–$I4/mcm$.

	M_o or C_o	T_o (K)	K
$KMnF_3$	0.022 (±0.001)	184.3 (±0.3)	0.4 (±0.12)
$KMn_{0.997}Ca_{0.003}F_3$	0.015 (±0.003)	185.3 (±0.2)	0.4 (±0.2)
$KMn_{0.983}Ca_{0.017}F_3$	0.000 93 (±0.000 09)	197.3 (±0.3)	0.8 (±0.3)
$KMn_{0.977}Ca_{0.023}F_3$	0.0052 (±0.0013)	201.5 (±0.5)	0.75 (±0.15)
C_{11}^S [a]	0.043 (±0.002)	184.5	0.43 (±0.03)
C_{44}^S [a]	0.000 83 (±0.000 05)	184.5	1.02 (±0.03)
$1/2(C_{11}^S - C_{12}^S)$ [a]	0.063 (±0.002)	184.5	0.50 (±0.03)
$1/2(C_{11}^S + C_{12}^S) + C_{44}^S$ [a]	0.016 (±0.001)	184.5	0.49 (±0.04)

[a] Calculated from the data in [16] as shown in figure 8(b).

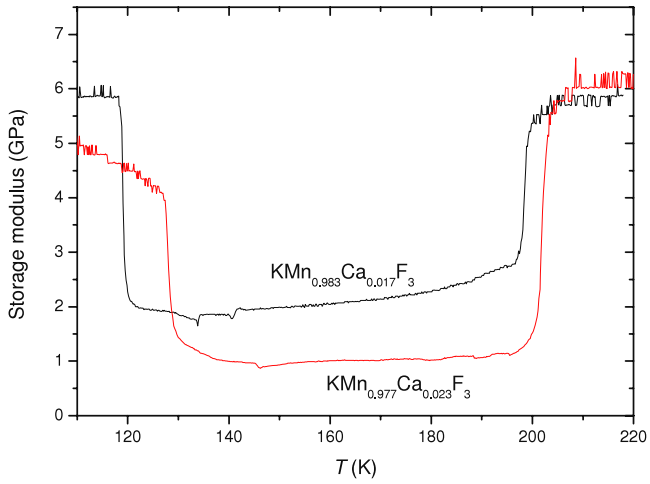

Figure 7. Storage moduli of $KMn_{0.983}Ca_{0.017}F_3$ and $KMn_{0.977}Ca_{0.023}F_3$ for $f = 1$ Hz.

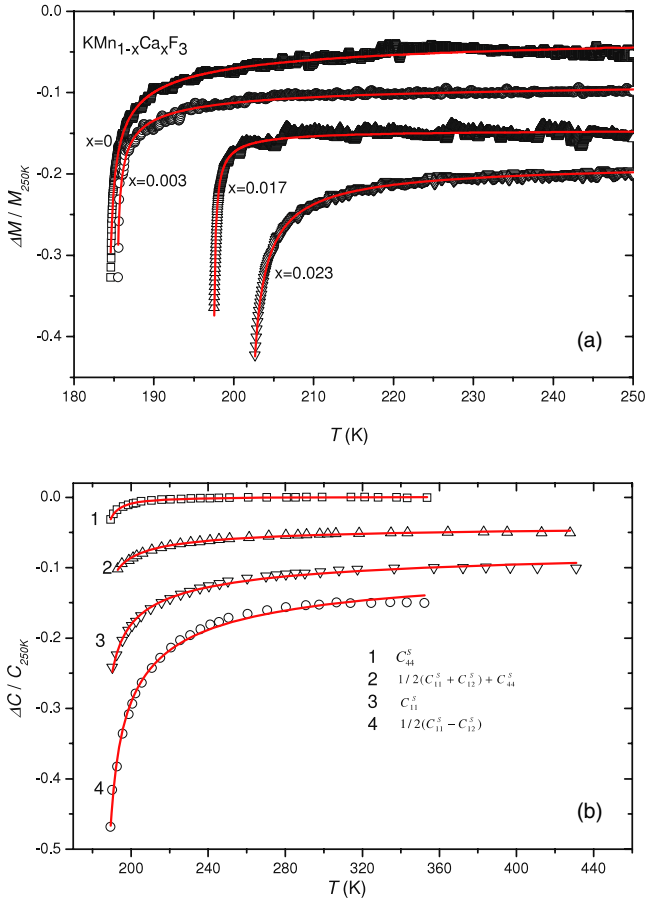

Figure 8. The relative softening of the storage modulus ($\Delta M/M_{250\,\mathrm{K}}$), elastic constants ($\Delta C/C_{250\,\mathrm{K}}$) and the fit to a power law. Elastic constants data for the $KMnF_3$ are extracted from data of Cao and Barsch [16]. The curves in (a) and (b) are shifted by 0.05 in the y-axis for clarity.

We analysed our own data and the data published in [16]. The value of ΔM is calculated as the difference between the experimental data and the baseline extrapolated from the high temperature data (see appendix A.17 in [24]). This value is then normalized with respect to the value at 250 K to obtain the relative softening of the moduli. Figure 8(a) shows the temperature dependence of the relative softening of the storage moduli above the tetragonal–cubic phase transition with $f = 8$ Hz. For clarity the various curves are stacked against each other, the high temperature limit is always zero. Softening was clearly observed within 10 K of T_o for all samples. A similar analysis of the high frequency elastic constants published by Cao and Barsch [16] is shown in figure 8(b). The temperature interval over which softening is observed is much greater for the high frequency data than for our low frequency observations.

The softening can be described empirically by a power law $[(T - T_o)/T_o]^{-K}$. The resulting fits to $\Delta M/M_{250\,\mathrm{K}} = -M_o[(T - T_o)/T_o]^{-K}$ or $\Delta C/C_{250\,\mathrm{K}} = -C_o[(T - T_o)/T_o]^{-K}$ are shown in figure 8; the parameters are listed in table 2. While the exponent is reasonably well constrained by the fit, the amplitudes M_o and C_o are less well determined and depend on the details of the experimental setting.

5. Discussion

The observed activation energy for the domain movement in $KMnF_3$ is 0.43 eV. This value is consistent with the activation energy of migration of the F vacancy in $KMnF_3$ [33, 34]. This indicates the relaxation process is due to the hopping of the F vacancy. No strong freezing of domain boundary movement was observed (no strong increase of the storage modulus under cooling in the tetragonal phase). The low value of the damping is seen as an indication that only few walls are

pinned even at our low frequency excitations and at relatively low temperatures. We may speculate that the low number of pinned domain walls may be due to the low concentration of the F vacancy and/or the fact that coupling between a domain wall and the F vacancy is not strong enough to pin the domain wall. A similar situation is encountered in $SrTiO_3$ where no domain wall freezing was observed down to the lowest temperature measured [6].

For $KMn_{0.997}Ca_{0.003}F_3$, the activation energy is 0.23 eV. The activation energy of the F interstitials in $KMnF_3$ simulated is 0.12 eV by Kilner [33] and 0.27 eV by Becher *et al* [34]. Our experimental value is consistent with the latter which may indicate that the related defects are F interstitials. As the ionic radius of the Ca^{2+} ions is larger than the Mn^{2+}, the Ca^{2+} ion forces the fluorine off its symmetry positions which may stabilize the (100) dumbbell fluorine interstitial.

It was reported that for $KMn_{0.997}Ca_{0.003}F_3$, domain wall freezing occurs at 107 K with activation energy of 0.15 eV [7], which may indicate that the related point defects are also fluorine interstitials. In our results, the hopping of the fluorine interstitial leads to a relaxation peak but cannot pin the domain wall. It is possible that the reported freezing is due to the Ca-(dumbbell fluorine interstitial) pairs. The fluorine dumbbell interstitial can rearrange its orientation around the Ca. When the rearrangement is frozen at low temperature, the domain wall is pinned at the same time. Schranz *et al* [7] reported that the freezing temperature shifts to higher temperature for higher Ca concentration which may also supports our hypothesis. Pinning in all other samples was too weak to allow a quantitative analysis.

Precursor softening exists in all samples. The exponent K, except for a higher value for C_{44}^S, varies between values of 0.4 ($\pm$0.2) and 0.8 ($\pm$0.3) with an overall mean value of 0.5. The lower values were found for $KMnF_3$, while K appears to increase with increasing Ca content. These values can be compared with the predictions of Carpenter and Salje [24] for fluctuation softening for D-dimensional phonon branches in the paraelastic phase (A35-A37 in [24]). The predicted exponent varies between 0.5 for three-dimensional softening, via 1 in the two-dimensional case, to 3/2 in the one-dimensional scenario. Our data, within experimental uncertainty, are consistent with a three-dimensional softening of phonon branches in the $Pm3m$ phase and clearly exclude lower-dimensional fluctuations.

In the extensive exploration of the high frequency ultrasonic response of $KMnF_3$ by Holt and Fossheim [35] similar exponents were found. The exponent 0.4 was reported for a limited temperature range while an exponent closer to 0.5 appeared possible over a larger temperature interval. Holt and Fossheim understood their experimental observations in terms of a 3D Heisenberg model based on the damping of the wave propagation at high frequencies. They referred explicitly to the behaviour of $SrTiO_3$ where Höchli and Bruce [23] found values of K ranging from 1.3 to 1.7. Höchli and Bruce stated that their data were quite inconsistent with the intrinsic behaviour of a Heisenberg or Ising model so that the influence of defects was evoked. Their values are much greater than in $KMnF_3$ so that it may be useful to consider why these two phase transitions, which appear to follow the same structural path, have such different exponents. Here we argue that the extend of the precursor softening in $KMnF_3$ and related compounds is strongly frequency dependent while the exponent K remains invariant. This could indicate that the coupling between the elastic response and the fluctuations are frequency dependent but that the dimensionality of the fluctuations is always 3. This analysis agrees with other interpretation of data within mean field behaviour of both materials [36–38]. It is also given support by the observation of short range order by hard mode spectroscopy by Bruce *et al* [39] which can be understood as a manifestation of the local structural deformation of the $Pm3m$ structure [40–43].

Acknowledgment

Support from Marie-Curie RTN Multimat (contract No. MRTN -CT-2004-505226) is acknowledged.

References

[1] Salje E K H 1993 *Phase Transitions in Ferroelastic and Co-Elastic Crystals* (Cambridge: Cambridge University Press)
Salje E K H 2008 *Phys. Chem. Minerals* **35** 321
[2] Harrison R J and Redfern S A T 2002 *Phys. Earth Planet. Inter.* **134** 253
[3] Harrison R J, Redfern S A T, Buckley A and Salje E K H 2004 *J. Appl. Phys.* **95** 1706
[4] Harrison R J, Redfern S A T and Salje E K H 2004 *Phys. Rev.* B **69** 144101
[5] Harrison R J, Redfern S A T and Street J 2003 *Am. Mineral.* **88** 574
[6] Kityk A V, Schranz W, Sondergeld P, Havlik D, Salje E K H and Scott J F 2000 *Phys. Rev.* B **61** 946
[7] Schranz W, Troster A, Kityk A V, Sondergeld P and Salje E K H 2003 *Europhys. Lett.* **62** 512
[8] Daraktchiev M, Salje E K H, Lee W T and Redfern S A T 2007 *Phys. Rev.* B **75** 134102
[9] Mercier O and Melton K N 1979 *Acta Metall.* **27** 1467
[10] Roytburd A L, Kim T S, Su Q M, Slutsker J and Wuttig M 1998 *Acta. Mater.* **46** 5095
[11] Lee W T, Salje E K H and Bismayer U 2005 *Phys. Rev.* B **72** 104116
[12] Wang C, Fang Q F, Shi Y and Zhu Z G 2001 *Mater. Res. Bull.* **36** 2657
[13] Lee W T, Salje E K H and Bismayer U 2003 *J. Appl. Phys.* **93** 9890
[14] Goncalves-Ferreira L, Redfern S A T, Artacho E and Salje E K H 2008 *Phys. Rev. Lett.* **101** 097602
[15] Lee W T, Salje E K H, Goncalves-Ferreira L, Daraktchiev M and Bismayer U 2006 *Phys. Rev.* B **73** 214110
Calleja M, Dove M T and Salje E K H 2003 *J. Phys.: Condens. Matter* **15** 2301
[16] Cao W and Barsch G R 1988 *Phys. Rev.* B **38** 7947
[17] Bruce A D and Cowley R A 1973 *J. Phys. C: Solid State Phys.* **6** 2422
[18] Stirling W G 1972 *J. Phys. C: Solid State Phys.* **5** 2711
[19] Slonczewski J C and Thomas H 1970 *Phys. Rev.* B **1** 3599
[20] Migoni R, Bilz H and Bäuerle D 1976 *Phys. Rev. Lett.* **37** 1155
[21] Fossheim K and Berre B 1972 *Phys. Rev.* B **5** 3292
[22] Fossheim K and Holt R M 1980 *Phys. Rev. Lett.* **45** 730
[23] Höchli U T and Bruce A D 1980 *J. Phys. C: Solid State Phys.* **13** 1963
[24] Carpenter M A and Salje E K H 1998 *Eur. J. Mineral.* **10** 693

[25] McKnight R E A, Howard C J and Carpenter M A 2009 *J. Phys.: Condens. Matter* **21** 015901
[26] McKnight R E A, Kennedy B J, Zhou Q and Carpenter M A 2009 *J. Phys.: Condens. Matter* **21** 015902
[27] Gibaud A, Shapiro S M, Nouet J and You H 1991 *Phys. Rev.* B **44** 2437
[28] Shirane G, Minkiewicz V and Linz A 1970 *Solid State Commun.* **8** 1941
[29] Hidaka M, Ohama N, Okazaki A, Sakashita H and Yamakawa S 1975 *Solid State Commun.* **16** 1121
[30] Kapusta J, Daniel P and Ratuszna A 1999 *Phys. Rev.* B **59** 14235
[31] Salazar A, Massot M and Oleaga A 2007 *Phys. Rev.* B **75** 224428
[32] Zhang H L, Wu X S, Chen C S and Liu W 2005 *Phys. Rev.* B **71** 64422
[33] Kilner J A 1981 *Phil. Mag.* A **43** 1473
[34] Becher R R, Sangster M J L and Strauch D 1989 *J. Phys.: Condens. Matter* **1** 7801
[35] Holt R M and Fossheim K 1981 *Phys. Rev.* B **24** 2680
[36] Salje E K H, Gallardo M C and Jimenez J 1998 *J. Phys.: Condens. Matter* **10** 5535
[37] Martin-Olalla J M, Romero F J, Ramos S, Gallardo M C, Perez-Mato J M and Salje E K H 2003 *J. Phys.: Condens. Matter* **15** 2423
[38] Romero F J, Gallardo M C, Hayward S A, Jimenez J, del Cerro J and Salje E K H 2004 *J. Phys.: Condens. Matter* **16** 2879
[39] Bruce A D, Taylor W and Murray A F 1980 *J. Phys. C: Solid State Phys.* **13** 483
[40] Salje E K H and Bismayer U 1997 *Phase Transit.* **63** 1
[41] Zhang M, Salje E K H, Bismayer U, Unruh H G, Wruck B and Schmidt C 1995 *Phys. Chem. Minerals* **22** 41
[42] Salje E K H, Ridgwell A, Guttler B, Wruck B, Dove M T and Dolino G 1992 *J. Phys.: Condens. Matter* **4** 571
[43] Salje E, Devarajan V, Bismayer U and Guimaraes D M C 1983 *J. Phys. C: Solid State Phys.* **16** 5233